JOURNAL OF MATERIALS SCIENCE 21 (1986) 2577–2580

Hydrostatic pressure dependences of elastic constants and vibrational anharmonicity of uranium nitride

M. D. SALLEH, J. E. MACDONALD, G. A. SAUNDERS
School of Physics, University of Bath, Claverton Down, Bath, BA2 7AY, UK
P. DE V. DU PLESSIS
Department of Physics, Rand Afrikaans University, PO Box 524, Johannesburg, South Africa

Measurements of the effect of hydrostatic pressure on ultrasonic wave velocities have been used to determine the pressure derivatives of the elastic stiffness of uranium nitride at room temperature. $\partial C_{44}/\partial P$, and hence the Grüneisen parameter for the transverse mode propagating down an $\langle 0\,0\,1\rangle$ axis, is negative; however, this mode softening is not anomalous for rocksalt structure crystals. The Grüneisen gammas of the acoustic modes obtained in the long wavelength limit have a pronounced anisotropy which accrues largely from the presence or absence of contributions to modes of vibration from nearest-neighbour repulsive forces. The compression of uranium nitride calculated from the Murnaghan equation of state is much smaller than those of the alkali halides or IV–VI compounds because this compound is much stiffer.

1. Introduction

To examine the anharmonicity of the long wavelength acoustic modes of uraniun nitride (UN) the effect of hydrostatic pressure upon its elastic constants has been measured. UN is one of the group of metallic uranium pnictide compounds which crystallize in the rocksalt structure. In the actinide metals and compounds both 6d and 5f electrons are involved in the chemical bond. Previously the elastic constants of UN have been measured as a function of temperature down through the Néel point $T_N(=53\,K)$ where marked anomalies occur, which have been interpreted in terms of spin–phonon interactions [1, 2]. This investigation of the elastic behaviour under the influence of hydrostatic pressure sheds further light on the difficult problem of the interatomic binding forces in uranium compounds.

2. Experimental procedures

Ultrasonic wave velocity measurements were made on a single crystal specimen having a pair of (1 1 0) faces polished flat and parallel to better than 10^{-4} rad. Ultrasonic pulses of fundamental frequency 10 MHz were generated and received in the single-ended technique by quartz transducers bonded to the crystal with Nonaq stop-cock grease. Pulse transit times were measured by the pulse echo overlap technique. The hydrostatic pressure dependences of the ultrasonic wave velocities were measured at pressures up to about 2×10^8 Pa in a piston and cylinder equipment using Plexol 201 as the pressure transmitting fluid.

3. Experimental results and discussion

The elastic constants obtained (Table I) are in reasonable agreement with those measured previously [1]. The second order elastic constants (SOEC) of UN are much greater than those of the alkali halides (for NaCl $C_{11}^S = 4.93$, $C_{12}^S = 1.30$, $C_{44}^S = 1.28$, $C'^S[=\frac{1}{2}(C_{11}^S - C_{12}^S)] = 1.82$, bulk modulus $B_0^S = 2.51$ units of $10^{10}\,Nm^{-2}$ [3]), the mixed covalent–ionic bonded lead and tin chalcogenide semiconductors (for PbTe $C_{11}^S = 10.53$, $C_{12}^S = 0.70$, $C_{44}^S = 1.322$, $C' = 4.91$, $B_0^S = 3.976$ in units of $10^{10}\,Nm^{-2}$ [4]) or even for the rare-earth chalcogenide SmS, which like UN contains a strong element of d- and f-binding ($C_{11} = 12.7$, $C_{12} = 1.2$, $C_{44} = 2.69$, $C' = 5.75$, $B_0^S = 5.03$ in units of $10^{10}\,Nm^{-2}$ [5]). Thus the interatomic binding forces in UN are particularly strong. In common with that of other rocksalt structure crystals, C_{11}, which includes a large contribution from the nearest-neighbour forces, is several times larger than C_{44}. For a more nearly ideally ionic crystal (such as NaCl) the forces are central so that the Cauchy relation ($C_{12} = C_{44}$) holds. The deviation, traditionally associated with covalency or a metal-like binding, from this relation is not particularly large in the case of UN. The acoustic mode velocities, found by solution of the Christoffel equations, are plotted as a function of mode propagation direction in Fig. 1.

The velocities of the longitudinal and two shear modes that are polarized in the [0 0 1] and [1 $\bar{1}$ 0] directions and propagated in the [1 1 0] direction were found to be linearly dependent upon the applied hydrostatic pressure (up to about 3×10^8 Pa). The hydrostatic pressure derivatives of the elastic stiffness constants C_{IJ} are given in Table II. These were calculated from the experimental data in the form of "natural" velocities W [6], using

0022–2461/86 $03.00 + .12

TABLE I The second order elastic stiffness constants (SOEC) for UN at 290 K.

Density ϱ_0 (kg m^{-3})	14 333
Lattice parameter a_0 ($\times 10^{-10}$ m)	4.89
Elastic stiffness constants	
C_{11} ($\times 10^{10}$ Nm^{-2})	42.39 ± 0.06
C_{12}	9.81 ± 0.09
C_{44}	7.57 ± 0.02
C' [$=\frac{1}{2}(C_{11} - C_{12})$]	16.29 ± 0.01
Anisotropy ratio C'/C_{44}	2.15
Bulk modulus B^S ($\times 10^{10}$ Nm^{-2})	20.67 ± 0.08
Volume compressibility χ^S ($\times 10^{-12}$ m^2 N^{-1})	4.82 ± 0.02
Linear compressibility ($\times 10^{12}$ m^2 N^{-1})	1.61
Elastic compliance constants	
S_{11} ($\times 10^{-12}$ m^2 N^{-1})	2.34
S_{12}	−0.72
S_{44}	1.32

TABLE II The hydrostatic pressure derivatives of the SOEC and bulk modulus of UN at room temperature (290 K) and atmospheric pressure.

$\partial C_{11}/\partial P$	9.97 ± 0.11
$\partial C_{12}/\partial P$	3.81 ± 0.14
$\partial C_{44}/\partial P$	−(0.74 ± 0.05)
$\partial C'/\partial P$	3.08 ± 0.25
$\partial B/\partial P$	5.86 ± 0.13
B_{11}	11.35
B_{12}	2.90
B_{44}	0.33
$C_{111} + 2C_{112}$	-72.3×10^{11} Nm^{-2}
$C_{123} + 2C_{112}$	-53.9×10^{11} Nm^{-2}
$C_{144} + 2C_{166}$	-2.4×10^{11} Nm^{-2}
Debye temperature θ_D^{el}	282 K
Mean Grüneisen parameter $\bar{\gamma}_H^{el}$	0.71
Thermal Grüneisen parameter γ^{th}	1.98

$$\left(\frac{\partial C_{IJ}}{\partial P}\right)_{T,P=0} = \frac{C_{IJ}}{C_{11}^T + 2C_{12}^T} + \frac{d}{dP}(\varrho_0 W^2)_{P=0} \quad (1)$$

where ϱ_0 is the density at atmospheric pressure. Also given in Table II are the hydrostatic pressure derivatives B_{IJ} of the thermodynamic second order elastic stiffness. In general for the rocksalt structure alkali halides and IV–VI compounds the pressure derivatives $(\partial C_{IJ}/\partial P)_{T,P=0}$ follow the trend $\partial C_{11}/\partial P > \partial C'/\partial P > \partial C_{12}/\partial P > \partial C_{44}/\partial P$ (see Table III of [4]). For UN as for these other crystals with the same structure, $\partial C_{11}/\partial P$ is by far the largest pressure derivative; this is because it is dominated by large contributions from nearest-neighbour repulsive terms and attractive terms including that from the Madelung energy. The normal trend is not followed in that $\partial C_{12}/\partial P > \partial C'/\partial P$. However, in all the compounds including UN $\partial C_{44}/\partial P$ is by far the smallest pressure derivative; that $\partial C_{44}/\partial P$ is negative for UN should not be viewed as anomalous — it is also negative for RbBr, KCl and KBr (but positive for NaCl, NaF and LiF). This negative $\partial C_{44}/\partial P$ reflects the negative sign of the Grüneisen parameter of the transverse mode propagated in the [0 0 1] direction, which can be accounted for structurally (see later).

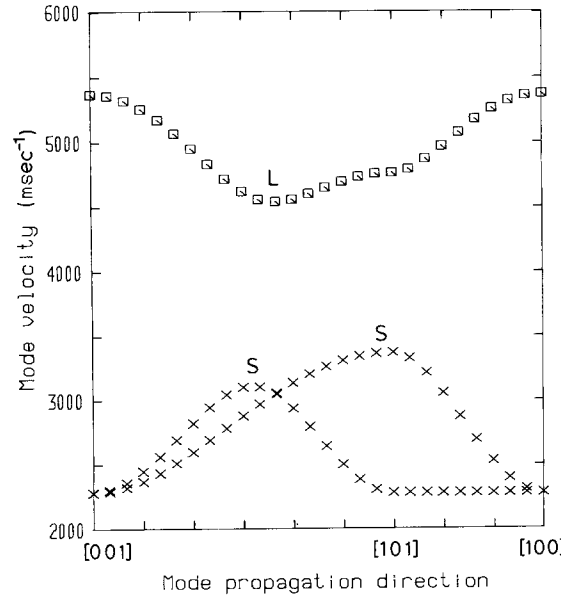

Figure 1 Acoustic mode velocity of UN as a function of mode propagation direction.

Knowledge of the compression $V(P)/V_0$ (the ratio of the volume $V(P)$ to the volume V_0 at atmospheric pressure) is central to theoretical studies of the physical properties of a crystal under pressure. To determine the effect of pressure on the volume, lattice parameter and nearest U–U distance, the Murnaghan [7] equation of state has been used in a logarithmic form

$$\ln\left(\frac{V_0}{V(P)}\right) = \frac{1}{B_0'^T}\ln\left[B_0'^T\left(\frac{P}{B_0^T}\right) + 1\right] \quad (2)$$

which describes the compression of many solids well [8]. Since ultrasonic measurements give adiabatic moduli, the data need to be transformed to the isothermal forms (Table III). Adiabatic B_0^S and isothermal B_0^T bulk moduli at temperature T are related by

$$B_0^S = B_0^T(1 + \alpha\gamma^{th}T). \quad (3)$$

Here γ^{th} (= 1.98 [9]) is the thermal Grüneisen parameter. The linear thermal expansion coefficient α_l is given by [9]

$$\alpha_l = 8.695 \times 10^{-6} + 12.343 \times 10^{-10}(T - 298) \quad (4)$$

so that the volume thermal expansion at 290 K is 26.06×10^{-6} (Table III). Using these values, $B_0'^T$ has been obtained as 20.36×10^{10} Nm^{-2}. The temperature derivative $(\partial B_0^T/\partial T)_P$ of the isothermal bulk modulus had been obtained using [8, 10]

$$\left(\frac{\partial B_0^T}{\partial T}\right)_P = \left(\frac{\partial B_0^S}{\partial T}\right)_P(1 + T\alpha\gamma) - \frac{B_0^S}{T}\left(\frac{T\alpha\gamma}{(1 + T\alpha\gamma)^2}\right)\left(1 + \frac{T(\partial\alpha/\partial T)_P}{\alpha}\right) \quad (5)$$

from measurements of B_0^S/T. The hydrostatic pressure derivative $(\partial B_0^T/\partial P)_T$ $(= B_0'^T)$ of the isothermal bulk modulus has then been calculated from [8, 10]

$$B_0'^T = B_0'^S + T\alpha\gamma\left(\frac{B_0^T}{B_0^S}\right) \times \left[1 - \left(\frac{2}{\alpha B_0^T}\right)\left(\frac{\partial B_0^T}{\partial T}\right)_P - 2B_0'^S\right] + \left[T\alpha\gamma\frac{B_0^T}{B_0^S}\right]^2\left[B_0'^S - 1 - \left(\frac{1}{\alpha^2}\right)\left(\frac{\partial\alpha}{\partial T}\right)_P\right] \quad (6)$$

TABLE III Primary thermodynamic data for UN at 290 K used for adiabatic (S) to isothermal (T) transformations

Bulk modulus $B_0^S = 20.67 \times 10^{10}\,Nm^{-2}$;	$B_0^T = 20.36 \times 10^{10}\,Nm^{-2}$
$\frac{\partial B_0^S}{\partial T} = -5.47 \times 10^7\,Nm^{-2}K^{-1}$;	$\frac{\partial B_0^T}{\partial T} = -6.47 \times 10^7\,Nm^{-2}K^{-1}$
$\frac{\partial B_0^S}{\partial P} (= B_0'^S) = 5.86$;	$\frac{\partial B_0^T}{\partial P} (= B_0'^T) = 6.06$
Volume thermal expansion coefficient $\alpha = 2.61 \times 10^{-5}\,K^{-1}$	$\frac{\partial \alpha}{\partial T} = 3.70 \times 10^{-9}$
Thermal Grüneisen parameter $\gamma^{th} = 1.98$ [9]	

The isothermal compression of UN calculated using the Murnaghan [7] equation of state (Equation 2) is plotted in Fig. 2. Previously the band structure and electronic pressure for UN have been computed in the lattice parameter range 4.75×10^{-10} to 4.90×10^{-10} m [11, 12]; using the compression obtained here, it is now possible to convert those results to the more experimentally direct effect of pressure on the uranium f and d, the nitrogen valence p electrons and the Madelung energy contributions to the band structure energy. In accord with its much stronger interatomic binding as evidenced by its much greater stiffness C_{IJ}, UN ($\Delta V/V_0 = 1.84\%$ at 40×10^8 Pa) has a much smaller compression than either the alkali halides ($\Delta V/V_0 = 1.8\%$ at 40×10^8 Pa for NaCl) or the mixed covalent–ionic lead chalcogenides ($\Delta V/V_0 = 8\%$ at 40×10^8 Pa for PbTe).

The three combinations $(C_{111} + 2C_{112})$, $(C_{123} + 2C_{112})$ and $(C_{144} + 2C_{166})$ of the third order elastic constants (TOEC), which can be determined from the hydrostatic pressure derivatives of the second order elastic constants, are given in Table II. The values show the same trends as the rocksalt structure alkali halides and IV–VI compounds (see Table IV of [4]), indicating that for UN, as for the other isostructural materials, C_{111} is by far the largest third order elastic constant. For an ionic Born–Mayer model with interaction potential between ions

$$\phi_{\mu\nu}(r) = (-Z^2e^2/r) + A \exp(-r/\varrho), \quad (7)$$

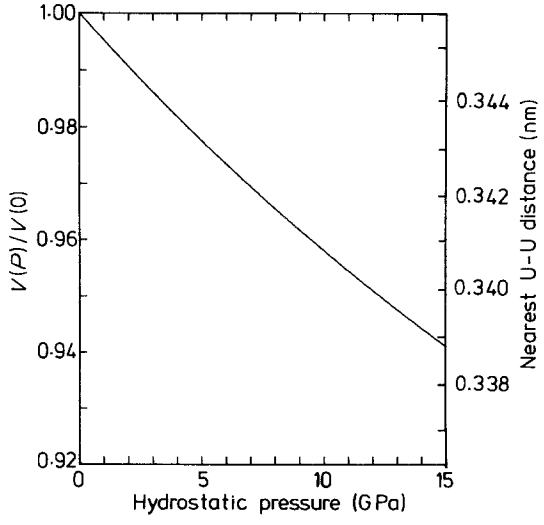

Figure 2 The isothermal compression of UN computed on the basis of the Murnaghan equation-of-state.

the forces would be central and the third order Cauchy relations [13] would be obtained giving

$$C_{123} = C_{456} = C_{144} = -10.4 \times 10^{11}\,Nm^{-2}$$
$$C_{112} = C_{166} = -4.0 \times 10^{11}\,Nm^{-2}$$

Although an ionic model cannot hold strictly for UN, it gives a useful indication of the relative magnitudes of the third order constants: C_{111} would be $-64 \times 10^{11}\,Nm^{-2}$. Including the contributions of repulsive terms up to second nearest neighbours, the TOEC C^0_{IJK} at 0 K are [14]

$$C^0_{IJK} = (C^0_{IJK})_{attractive} + (C^0_{IJK})_{repulsive} \quad (8)$$

$$C^0_{111} = 10.2639\frac{Z^2e^2}{r_0^4} - \frac{\psi(r_0)}{\varrho}\left(\frac{3}{r_0^2} + \frac{3}{\varrho r_0} + \frac{1}{\varrho^2}\right) - \frac{\psi(2^{1/2}r_0)}{2\varrho}\left[\frac{3(2)^{1/2}}{r_0^2} + \frac{6}{\varrho r_0} + \frac{2(2)^{1/2}}{\varrho^2}\right] \quad (9)$$

$$C^0_{112} = C^0_{116} = -1.2086\frac{Z^2e^2}{r_0^4} - \frac{\psi(2)^{1/2}r_0}{4\varrho} \times \left[\frac{3(2)^{1/2}}{r_0^2} + \frac{6}{\varrho r_0} + \frac{2(2)^{1/2}}{\varrho^2}\right] \quad (10)$$

$$C^0_{123} = C^0_{456} = C^0_{144} = 0.6784\frac{Z^2e^2}{r_0^4} \quad (11)$$

In the case of C^0_{111} the second term, due to the nearest-neighbour repulsion, is about two orders of magnitude greater than the third term, which results from repulsion between next nearest-neighbours, and can be neglected. Hence C_{111} has a large and negative value because it is dominated by the nearest-neighbour repulsion (this will also be true for the mixed ionic–covalent bonding closer to the real situation in UN). In the ionic model the nearest–neighbour term does not contribute to the other third order elastic constants, so that these are much smaller than C_{111}.

4. Long wavelength acoustic mode Grüneisen parameters of UN

Knowledge of the elastic constants and their hydrostatic pressure derivatives enables the Grüneisen gammas $\gamma(p, N)$ of the acoustic modes in the long wavelength limit to be calculated. In the anisotropic continuum model the $\gamma(p, N)$ for cubic crystals are given by [15]

$$\gamma(p, N) = (1/6w)(3B + 2w + k) \quad (12)$$

where

$$w(p, N) = C_{11}K_1 + C_{44}K_2 + C_{12}K_3 \quad (13)$$

$$k(p, N) = C_1K_1 + C_2K_2 + C_3K_3 \quad (14)$$

with

$$K_1(p, N) = N_1^2U_1^2 + N_2^2U_2^2 + N_3^2U_3^2 \quad (15)$$

$$K_2(p, N) = (N_2U_3 + N_3U_2)^2 + (N_3U_1 + N_1U_3)^2 + (N_1U_2 + N_2U_1)^2 \quad (16)$$

$$K_3(p, N) = 2(N_2N_3U_2U_3 + N_3N_1U_3U_1 + N_1N_2U_1U_2) \quad (17)$$

$$C_1 = C_{111} + 2C_{112} \quad (18)$$

$$C_2 = C_{144} + 2C_{166} \quad (19)$$

$$C_3 = C_{123} + 2C_{112} \quad (20)$$

Here N_i and U_i are direction cosines for wave propagation and polarization directions. The $\gamma(p, N)$ have been computed as a function of mode propagation direction, the mode velocities being obtained from the solutions plotted in Fig. 1. The acoustic mode Grüneisen parameters in directions in the symmetry planes normal to the twofold and fourfold directions are plotted in Fig. 3. These Grüneisen parameters quantify the first order anharmonicity of the acoustic modes at the Brillouin zone centre. The marked anisotropy of these $\gamma(p, N)$ can be understood in terms of the types of acoustic modes which can propagate in the rocksalt structure and their relationship to the interionic forces, in particular when nearest-neighbour repulsion plays a role. Consider for example the $\gamma(p, N)$ for modes propagating along a four-fold $\langle 0\,0\,1\rangle$ direction. Inspection of the mode gamma equations shows that the longitudinal mode $\gamma(p, N)$ has a comparatively large positive value (+2.2) because the third order elastic constant combination $(C_{111} + 2C_{112}) = C_1 = -72.3 \times 10^{11}\,\mathrm{Nm}^{-2}$ (Table II) is large and negative. Hence $C_1K_1 = -72 \times 10^{11}\,\mathrm{Nm}^{-2}$ (K_1 being for the longitudinal mode) is much greater than $w(=C_{11}K_1 = +4.239 \times 10^{11}\,\mathrm{Nm}^{-2})$, and so dominates $\gamma(p, N)$. Now $(C_{111} + 2C_{112})$ is in turn largely determined by C_{111}: the nearest-neighbour repulsion is responsible for the substantial value of $\gamma(p, N)$ for the longitudinal $q[0\,0\,1]$ acoustic mode. In contrast C_{111} is not involved in Grüneisen gamma for the shear acoustic wave propagated along an $\langle 0\,0\,1\rangle$ direction – for this mode the nearest-neighbour forces do not come into play. This mode comprises a vibration in which the (0 0 1) planes of atoms vibrate almost as a unit perpendicular to the direction of the nearest-neighbour bonds, and since all the changing bond lengths increase, the Grüneisen parameter is negative (Fig. 3). The thermodynamic properties of the crystal at low temperatures (including the thermal expansion) should be determined by the dominance of the phonon population in this transverse low lying branch. In general application of the principle that when C_{111} is involved then the nearest-neighbour repulsion will be important in determining the vibrational anharmonicity accounts for the marked anisotropy of the acoustic mode Grüneisen parameter of UN.

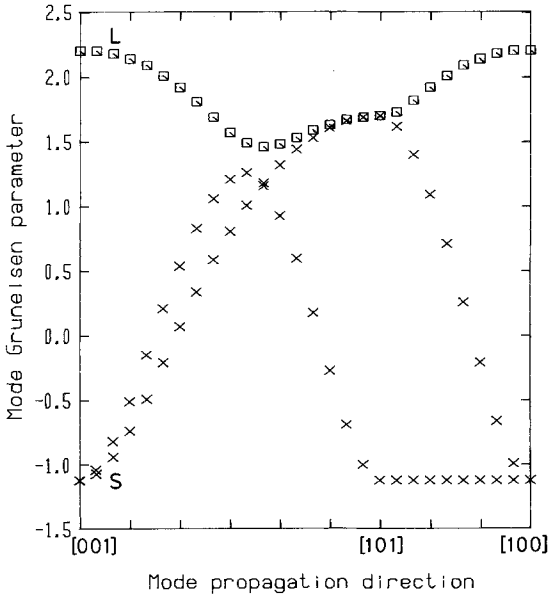

Figure 3 The acoustic mode Grüneisen parameter $\gamma(p, N)$ in the long wavelength limit as a function of mode propagation directions in UN.

To obtain a mean high temperature acoustic mode Grüneisen parameter, the expression

$$\bar{\gamma}_H^{el} = \frac{1}{3N}\Sigma\gamma(p, N) \quad (21)$$

has been summed over a grid of 10 288 points in velocity space for equal elements of solid angle centred on each propagation vector N. At room temperature UN nears the high temperature limit ($T > \theta_D = 282$ K (Table II)) so Equation 21 is a reasonable approximation. The value of $\bar{\gamma}_H^{el}$ (=0.71) obtained (Table II) is substantially smaller than the thermal Grüneisen parameter γ^{th} (= 1.98), which indicates that the mean of the Grüneisen parameters for optic mode and for acoustic modes away from the Brillouin zone centre is much larger than that for the zone centre acoustic modes.

References

1. C. F. VAN DOORN and P. DE V DU PLESSIS, *J. Magn. Magn. Mater.* **5** (1977) 164.
2. R. H. LEMMER and J. DE P. VILJOEN, *ibid.* **5** (1977) 161.
3. S. HART, *J. Phys. D.* **1** (1968) 1277.
4. A. J. MILLER, G. A. SAUNDERS and Y. Y. YOĞURTÇU, *J. Phys. C.* **14** (1981) 1569.
5. Tu. HAILING, G. A. SAUNDERS and H. BACH, *Phys. Rev.* **B29** (1984) 1848.
6. R. N. THURSTON and K. BRUGGER, *ibid.* **133** (1964) A1604.
7. F. D. MURNAGHAN, *Proc. Nat. Acad. Sci. USA* **30** (1944) 244.
8. O. L. ANDERSON, *J. Phys. Chem. Solids* **27** (1966) 547.
9. A. C. MOMIN and M. D. KARKHANAVALA, *High Temp. Sci.* **11** (1979) 179.
10. W. C. OVERTON, *J. Chem. Phys.* **37** (1962) 116.
11. M. S. S. BROOKS and D. GLÖTZEL, *Physica* **102B** (1980) 51.
12. M. S. S. BROOKS, *J. Phys. F: Met. Phys.* **14** (1984) 639.
13. C. S. G. COUSINS, *J. Phys. C.* **4** (1971) 1117.
14. K. P. THAKUR, *J. Phys. Chem. Solids* **41** (1980) 465.
15. K. BRUGGER and T. C. FRITZ, *Phys. Rev.* **157** (1967) 524.

Received 23 August
and accepted 3 October 1985